Dent Res Oral Health 2019; 2(2): 003-016 DOI: 10.26502/droh.007

Research Article

# Biomechanical Study of Implant Treatment For Maxillas With Different Bone Quality

**Takaaki Arahira[1], Mitsugu Todo[2]**

[1]Faculty of Management and Information Science, Kyushu Institute of Information Sciences, 6-3-1 Saifu, Dazaifu 818-0117, Japan

[2]Research Institute for Applied Mechanics, Kyushu University, 6-1 Kasuga-koen, Kasuga 816-8580, Japan

***Corresponding Author:** Takaaki Arahira, Faculty of Management and Information Science, Kyushu Institute of Information Sciences, 6-3-1 Saifu, Dazaifu 818-0117, Japan, E-mail: arahira@kiis.ac.jp

**Received:** 12 June 2019; **Accepted:** 24 June 2019; **Published:** 27 June 2019

## Abstract

**Purpose:** The purpose of this study is to characterize the effects of the implant treatment on the distribution of the strain energy density in the maxillas using finite element analysis.

**Methods:** Three-dimensional maxillary bone models of a male and a female patient were constructed using their CT-images. The distributions of Young's modulus were estimated from their bone mineral density distributions. Total six implants were embedded into each of the maxillary models. Finite element analysis of the maxilla models was then performed in order to assess the concentrations of the strain energy density, especially in the vicinity of the embedded implants under the two different loading conditions.

**Results:** In both models, strain energy density was concentrated especially around the right-molar implant, suggesting the outbreak of damage and subsequent absorption of bone tissue in this region. The female model with smaller size and lower bone density exhibited much higher localized concentration of the strain energy density than the male model. Therefore, a modified placement of the right-molar implant was then introduced into the female model and such high concentration was effectively reduced by using the inclined and longer implant.

**Conclusion:** This kind of three-dimensional modeling can clinically be used to predict the optimal implant treatment for each of dental patients.

Dent Res Oral Health 2019; 2(2): 003-016 DOI: 10.26502/droh.007

**Keywords:** Dental Biomechanics; CT-Image Based Modeling; Finite Element Analysis; Bone Quality; Strain Energy Density

## 1. Introduction

In the case of implant treatment, four to eight implants were treated for a patient with edentulous maxilla or mandible [1-3], depending on the bone density and structural stability of the patient. Thus, occlusal forces during daily activities and unexpected forces such as bruxism [4,5] are supported by those inserted implants and the mechanical stresses were directly transmitted into the jaw bones. In the case of bruxism, the buccal mandibular movement causes the risk of implant fracture as the result of the bending overload [5]. It is therefore expected that a jaw bone with implants is facing much severer mechanical situations than a jaw bone with teeth. This kind of mechanical stress has been considered to cause bone absorption around the implants [6-8], resulting in the loosening and the subsequent removing of the implants. Therefore, finite element analysis of jaw bones with implants has actively been conducted in order to understand such mechanical conditions in the vicinity of the implants [9-10].

In the computational analysis of jaw bones, mandibles have mainly been investigated by constructing their three-dimensional models [11-15] and few attempts have been made to assess maxillas computationally. In general, structure of maxillas is more complex than that of mandibles [16], and it makes resulting in an increase of the risk of the surgical treatments [17]. For example, hollow structures named sinus maxillaries exist in the maxilla, and the bone tissue under the sinus is thin structure that makes the placement of implants difficult. In the vicinity of sinus maxillaries, an implant is usually tried to be inserted into the rear or front part of the sinus maxillaries, or inclined to avoid the sinus maxillaries.

In the field of computational mechanics, CT-image based modeling has actively been developed to construct the models of detailed bone structures considering their three-dimensional shapes, and has effectively been applied to the clinical problems in orthopedics [18-21] and dentistry [22-28]. In this modeling procedure, detailed bone models are constructed from CT-images by extracting the cross-sectional areas corresponding to the bones. Furthermore, the remodeling mechanism has been tried to be simulated by using various theoretical approaches in the bone tissue [29-34]. These approaches can be divided into two categories, macroscopic and microscopic approaches. One of the macroscopic approaches is based on a mechanical hypothesis in which the bone remodeling can be controlled by strain energy density [29-31,33]. On the other hand, one of the microscopic approaches tries to understand the remodeling mechanism by using the biomechanical responses of bone tissue related osteocytes [34].

In this study, two different types of maxilla models varying in the shape and the bone quality were constructed using the CT images of the edentulous maxilla of a male and a female patient. Total six implants were inserted into each of the maxilla models. Finite element analysis was performed to assess the effects of the implant treatment on the distribution of the strain energy density in the maxillas.

## 2. Materials and methods

### 2.1 Finite element models and analysis

Two different types of maxilla models were constructed by using the CT images of the jaw bones of an 84 years old male and a 65 years old female. The total number of the CT images and the slice distance were 80 and 0.5 mm for the male and 37 and 1 mm for the female. Mechanical Finder (RCCM, Inc.), a software for finite element modeling and analysis of bone structure, was used in this study. Four-nodes tetrahedral elements were used to construct a finite element model of the maxilla. The total number of elements and nodes were 134223 and 630675 for the male model and 110052 and 505919 for the female model. Figure 1 shows the three-dimensional solid models. The models had the limited upper and side boundaries because only the limited regions of maxilla in which implants were supposed to be inserted were chosen by the dentist in charge and taken by CT in order to minimize the effects of X-ray radiation to the patients.

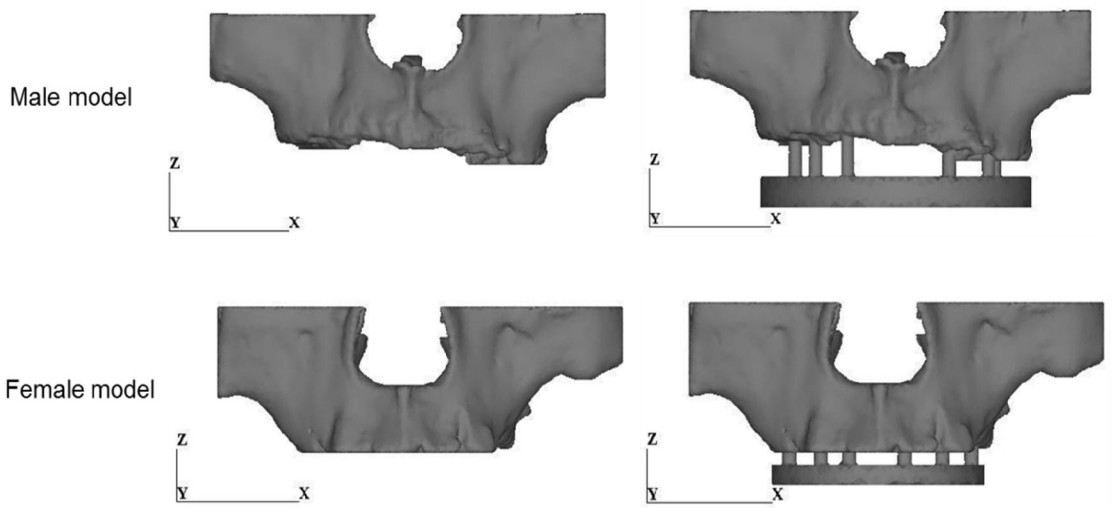


**Figure 1:** Computational models. The upper side is 84 years old male model, the lower side is 65 years old female model. The left side is a finite element model of edentulous maxilla, the right side is maxilla models with prosthesis.

The bone mineral density, ρ, corresponding to each element was estimated from the averaged CT value (Hounsfield units) using the following formula [35]:

$\rho\ (g/cm^3) = (CT\ value + 1.4246) \times 0.001/1.0580$ for CT value > -1 (1)

$\rho(g/cm^3) = 0.0$ for CT value ≤ -1 (2)

The Young's modulus of the element was then calculated from the corresponding bone density by using the relationship by Keyak, et al. shown in Table 1 [18].

| Bone density [g/cm$^3$] | Young's modulus [MPa] |
|---|---|
| $\rho=0$ | $E=0.001$ |
| $0<\rho\leqq0.27$ | $E=33900\rho^{2.20}$ |
| $0.27<\rho\leqq0.6$ | $E=5307\rho+469$ |
| $0.6\leqq\rho$ | $E=10200\rho^{2.01}$ |

**Table 1:** Relationship between bone density and Young's modulus [18].

For each maxilla model, a prosthesis model consisting of six implants and a curved support was developed as shown in Figure 2. The diameter of all implants was chosen to be 3.75mm. The curved supports were determined so that they fitted to the curved shapes of the maxillas. The material of the implant and the curved support was assumed to be pure titanium with the Young's modulus of 106 GPa and the Poisson's ratio of 0.3. Figure 1 shows these prosthesis models were attached to the maxilla models. In a real structure of maxilla, gingiva usually exists in the space between the maxilla and the curved support and neglected in this modeling. The boundaries between maxilla and implants were assumed to be perfectly bonded. The length of each implant was set to be maximized in each implantation position as shown in Table 2. In Table 2, the number in the parenthesis expresses the insertion length of the implant within maxilla.

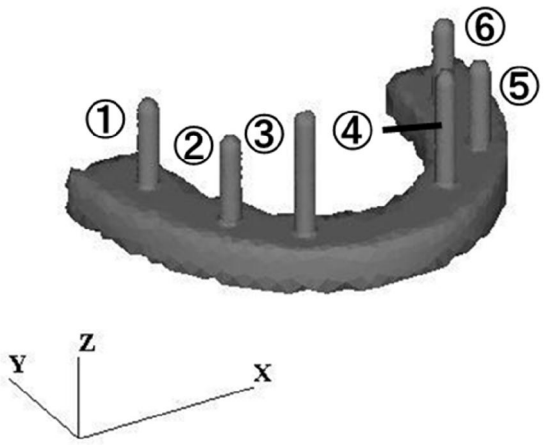


(a) 84 years old male

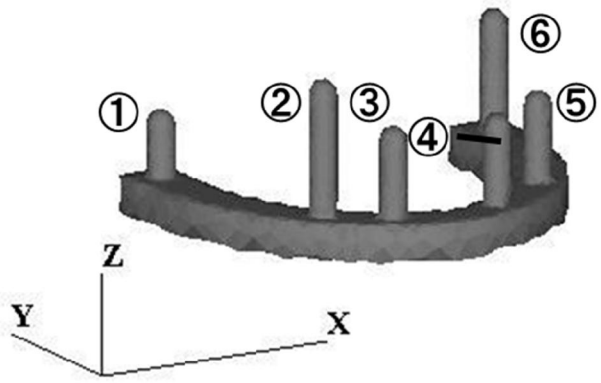


(b) 65 years old female (original model)

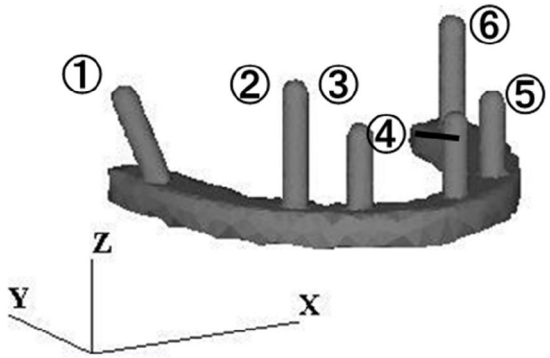


(c) 65 years old female (modified model)

**Figure 2:** Prosthesis models consisting of implants and curved support.

| **Implant No** | | ① | ② | ③ | ④ | ⑤ | ⑥ |
|---|---|---|---|---|---|---|---|
| Length [mm] | Male | 16 (7.2) | 16 (8.6) | 22 (12.1) | 21 (15.7) | 16 (12.1) | 16 (11.7) |
| | Female | 9 (6) | 18 (14.9) | 12 (8.9) | 12 (9) | 12 (9) | 16 (11.9) |

**Table 2:** Length of each implant. The number in parenthesis is the insertion length.

Figure 3 shows the boundary condition. In the restraint condition, the top of the maxilla model was totally fixed as shown in Figure 3(a). In the loading condition I, a distributed load of 200N was applied to the bottom surface of the prosthesis in the +Z-direction as shown in Figure 3(b). The value of 200N has been reported as an actual load

subjected to jaw bones during an occlusion condition [36]. In the loading condition II, a partially distributed load of 100N was applied to the left half surface of the prosthesis in the +X-direction as shown in Figure 3(c). It is noted that the horizontal loading simulates a bruxism condition.

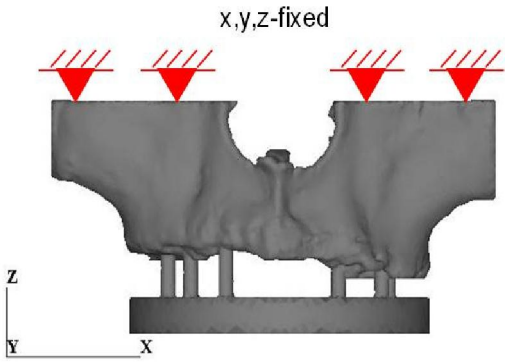


(a) Restraint condition

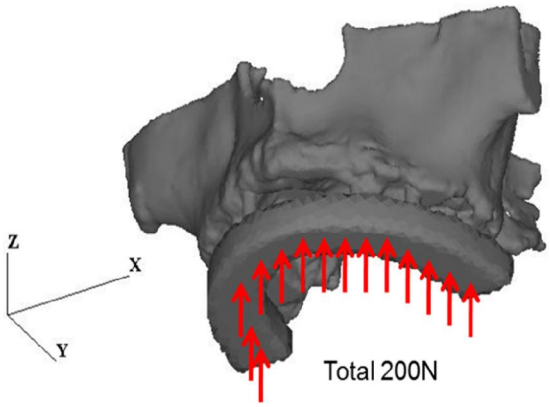


(b) Loading condition I

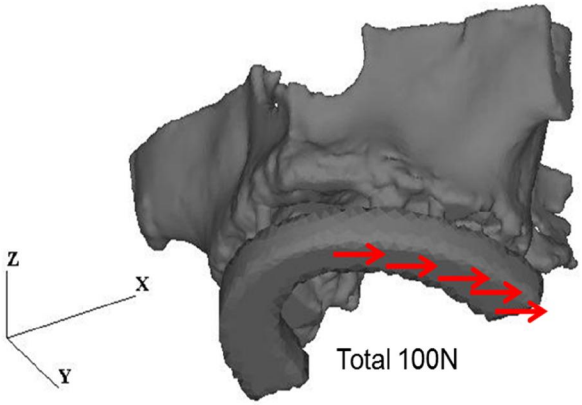


(c) Loading condition II

**Figure 3:** Boundary conditions applied to maxilla model.

## 3. Results

### 3.1 Distribution of Young's modulus

Figure 4 shows the distributions of Young's modulus on the vertical cross-sectional areas at the implant ①. It is clearly observed that higher moduli were distributed in the cortical bone regions. It is also noted that the female model exhibited lower modulus than the male model. The variations of the modulus along the dashed lines A-A' and B-B' are plotted in Figure 6. One modulus value was plotted at each element along the lines. It is clearly seen that higher moduli were distributed in the cortical bone regions and the female model exhibited much lower distribution of the modulus than the male model.

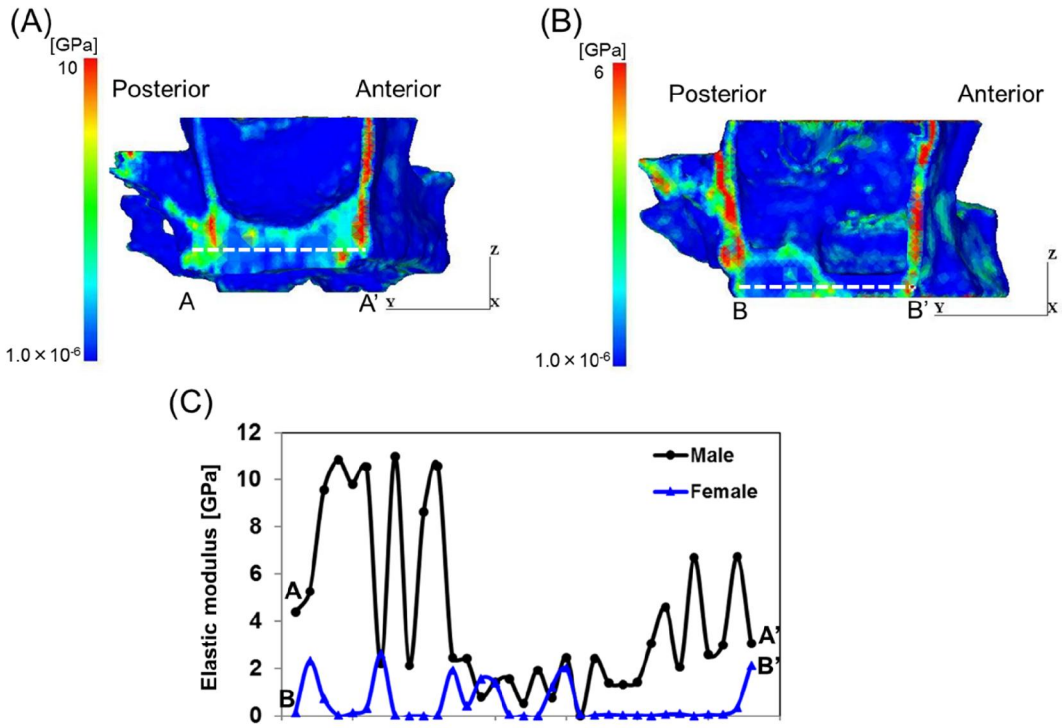


**Figure 4:** Elastic modulus of finite element model. (A) is 84 years old male model. (B) is 65 years old female model. (C) is distribution of elastic modulus along each dashed line in (A) and (B).

### 3.2 Distribution of strain energy density

Figure 5 shows the maximum values of the strain energy density in maxilla in the vicinity of the implants. In the case of loading condition I, for both models, the highest maximum value existed in the vicinity of the implant ①. Compared with the maximum value of the strain energy density in the implant ①, there was a 68.8% difference between male and female model. Similarly, in the case of loading condition II, the highest maximum value existed in the implant ①, and then, three implants (implant ①, ②, ③) were most affected. However, for both models, the maximum values in the implant ② and ③ are smaller than that of the implant ①. Compared with maximum value in the implant ①, there was a 67.3% difference between male and female model. In the case of the female model,

the length of the implant ① was the shortest (see Table 2) and the distance between the implant ① and ② was the longest (see Figure 2(b)), therefore the implant ① was influenced by higher load and moment than the others. In the case of the male model, on the other hand, the insertion length of the implant ① was the shortest as shown in Table 2 because of the shorter width of the right-side bone than the left-side as shown in Figure 1(a). This shortest insertion length of implant might cause the highest strain energy density.

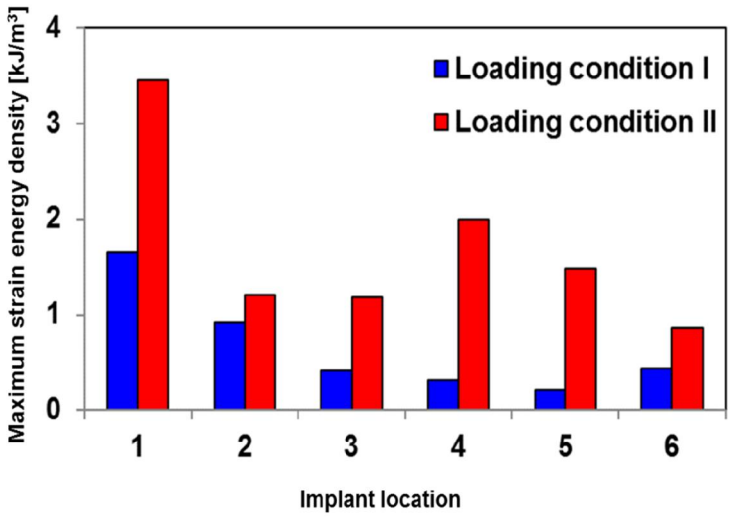


(a) 84 years old male.

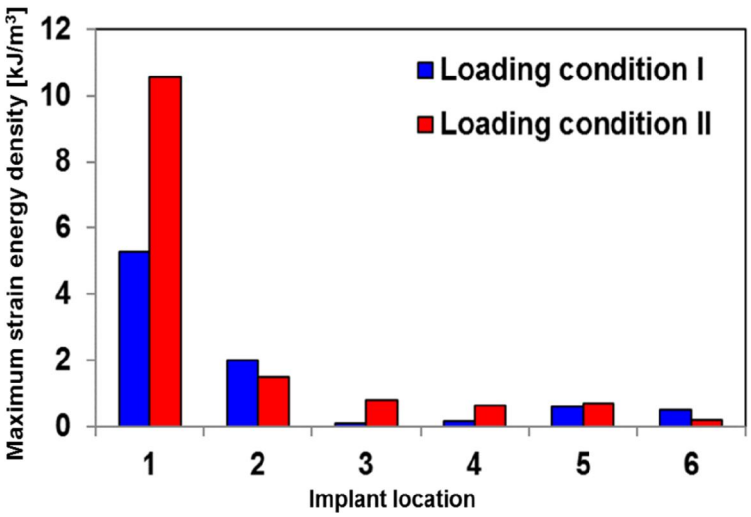


(b) 65 years old female.

**Figure 5:** Comparison of maximum strain energy density in the vicinity of implants.

The distribution of strain energy density in the cross-sectional areas of the implants ① for a male and female model is shown in Figure 6. It is clearly seen that the distribution of the strain energy density was mainly concentrated around the inserted implants.

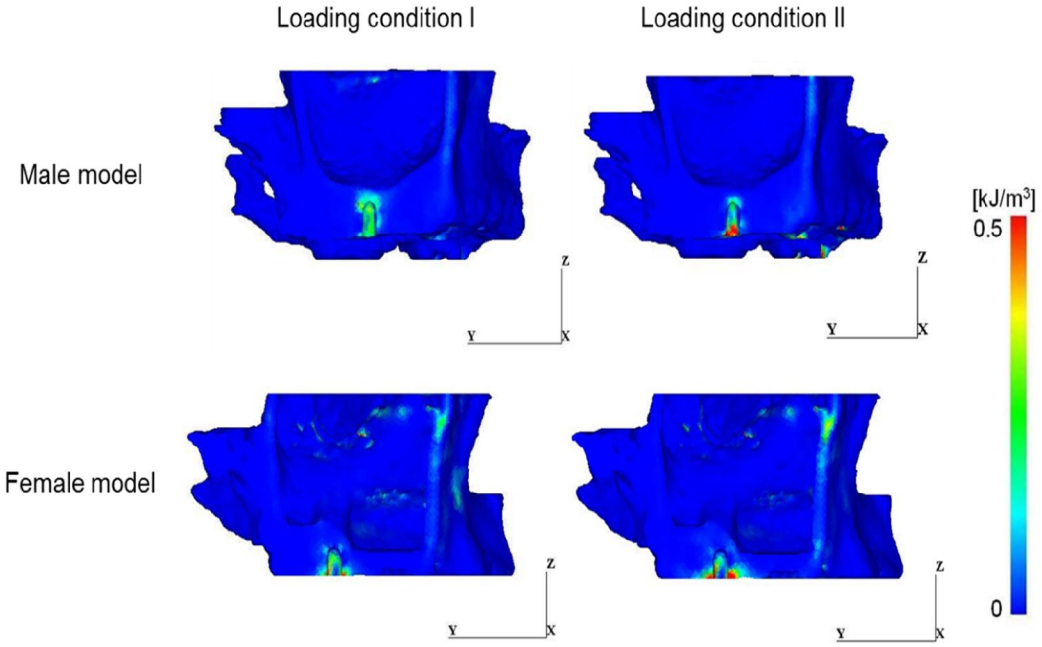


**Figure 6:** Distribution of strain energy density in the vicinity of the right molar implant. The upper side is 84 years old male model, the lower side is 65 years old female model. The left side is loading condition I, the right side is loading condition II.

## 4. Discussion

In the female model, the implant ① exhibited higher strain energy density than that of the male model. Considering the lower bone density and weak bone structure of the female model, such high concentration of the strain energy density may cause damage and subsequent bone absorption around the implant ①. It is recommended to modify the implant ① to reduce the concentration of the strain energy density. One of the effective approaches is thought to lengthen the implant ①, however, the sinus maxillaries located above the implant prevents such lengthening. Therefore, an inclined insertion of implant was applied to the model. Figure 2(c) shows the modified prosthesis model introduced to the female model. The length of the implant was changed from 9 to 15 mm, and it was inclined by 45 degree to avoid the sinus maxillaries.

Figure 7 shows the maximum strain energy density in the vicinity of each implant. It is clearly observed that the strain energy density around the implant ① was dramatically reduced by the modified female model. It is successful that the maximum value of the strain energy density in the implant ① under the loading condition I and II decreased 75.4%, 45.7% by being modified the implant ①, respectively. Figure 8 shows the distribution along the indicated

lines around the implant ①. It is noted that the distribution in the modified female model was comparable to that in the male model.

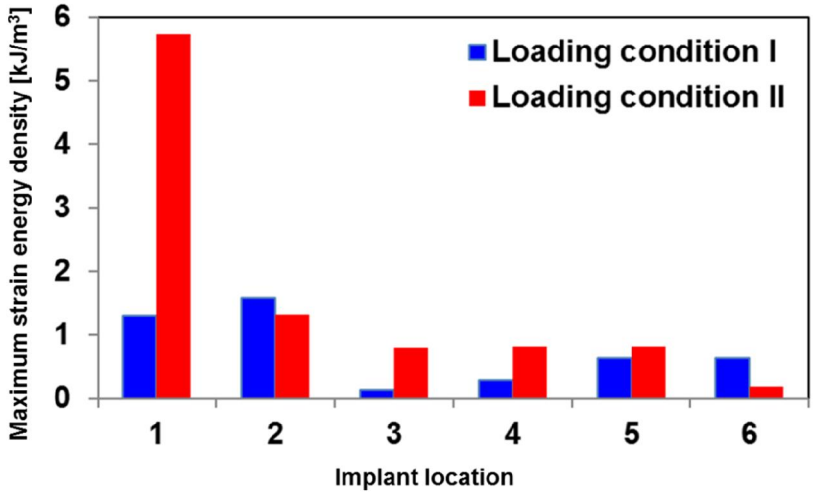


**Figure 7:** Maximum strain energy density in the vicinity of implants of modified model.

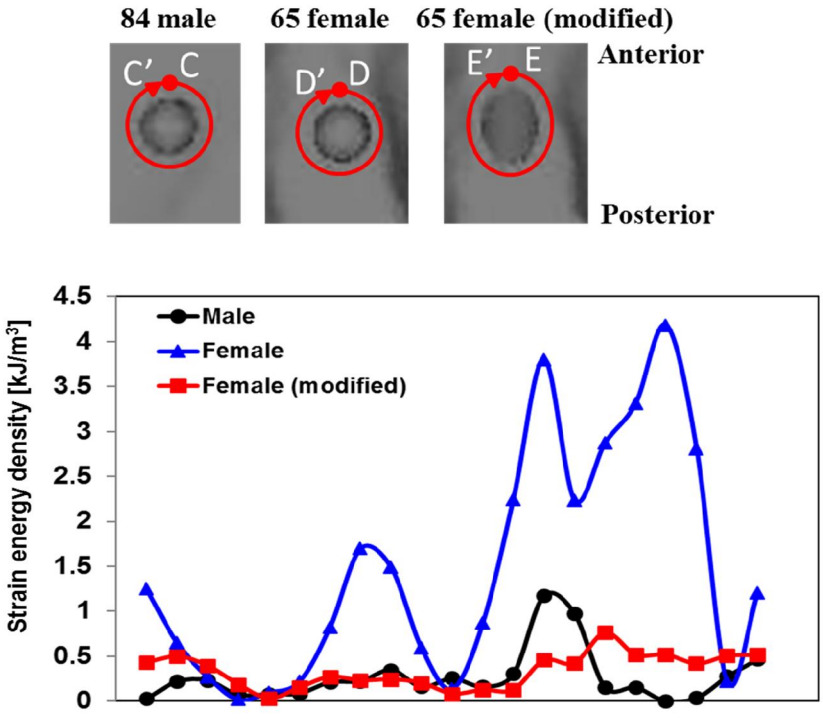


(a) Loading condition I

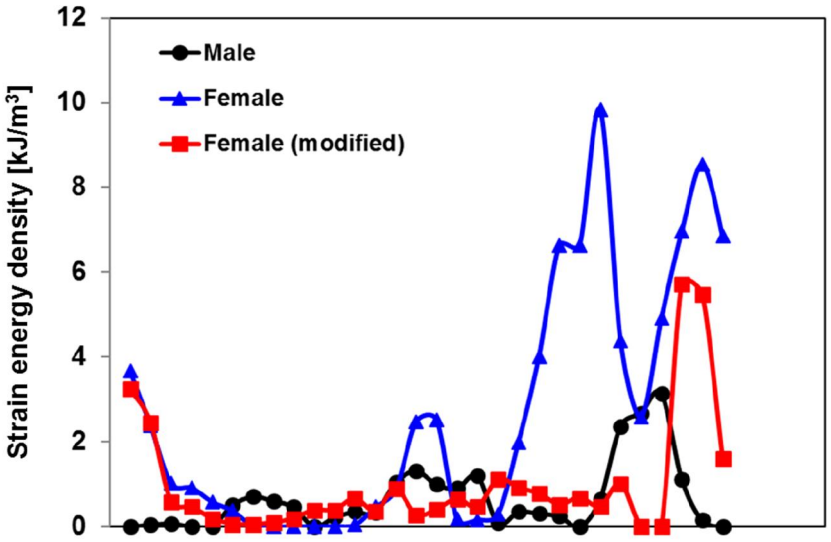


(b) Loading condition II

**Figure 8:** Distribution patterns of strain energy density along the lines around the implant ①.

It should be noted that lengthened and inclined implant effectively improves the safety of the implant treatment; however, much higher surgical skill is required for the dentist. It is also noted that in an actual implant treatment, the number of the implants may unwillingly be reduced due to the structural weakness of the maxilla. Therefore, risk assessment by the computational method is recommended to minimize the number of the implants and to optimize the positions and the lengths of the implants for patients.

In actual medical treatments, threshold level of strain energy density could be very useful in order to predict the risk assessment for bone absorption using the computational analysis during the preoperative planning. Further study needs to be done to find such threshold level and establish the computer aided preoperative procedure.

## 5. Conclusion

Three-dimensional finite element models of edentulous maxillas of a male and female patient were developed using their CT-images. For each model, a prosthesis model, including six-implants and a curved support was attached to the maxilla. Finite element analysis was then performed to assess the effects of the implantation on the concentration of the strain energy density that has been considered to be a macroscopic parameter controlling bone absorption around the implants. The conclusions are summarized as follows:

(1) In both the maxilla models, strain energy density was severely concentrated around the implant ①, and the concentration in the female model was higher than in the male model, suggesting bone absorption around the implant ① of the female model.

(2) The high concentration of the strain energy density around the implant ① was thought to be attributed to the shortest insertion length of the implant, resulting in the smallest contact area with bone tissue. For the female model,

furthermore, the longer distance between the implants ① and ② was also considered to result in the higher moment subjected to the implant ①.

(3) The implant ① of the female model was replaced by a longer and inclined implant. The concentration of the strain energy denisty was then successfully reduced.

## 6. Funding

This research did not receive any specific grant from funding agencies in the public, commercial, or not-for-profit sectors.

## References

1. Sadowsky SJ, Treatment considerations for maxillary implant overdentures: A systematic review. J Prosthet Dent 97 (2007): 340-348.
2. Turkyilmaz I, Company AM, McGlumphy EA, Should edentulous patients be constrained to removable complete dentures? the use of dental implants to improve the quality of life for edentulous patients. Gerodontology 27 (2010): 3-10.
3. Carlsson GE, Omar R, The future of complete dentures in oral rehabilitation. A critical review. J Oral Rehabil 37 (2010): 143-56.
4. Kinsel RP, Lin D, Retrospective analysis of porcelain failures of metal ceramic crowns and fixed partial dentures supported by 729 implants in 152 patients : Patient-specific and implant-specific predictors of ceramic failure. J Prosthet Dent 101 (2009): 388-94.
5. Cornad, HJ, Schulte JK, Vallee MC, Fractures related to occlusal overload with single posterior implants: a clinical report. J Prosthet Dent 99 (2008): 251-256.
6. Isidor F, Loss of osseointegration caused by occlusal load of oral implants. A clinical and radiographic study in monkeys. Clin Oral Implants Res 7 (1996): 143-152.
7. Isidor F, Histological evaluation of peri-implant bone at implants subjected to occlusal overload or plaque accumulation. Clin Oral Implants Res 8 (1997): 1-9.
8. Matarasso S, Salvi GE, Iorio Siciliano V, Cafiero C, Blasi A, Lang NP, Dimensional ridge alterations following immediate implant placement in molar extraction sites: A six-month prospective cohort study with surgical re-entry. Clin Oral Implants Res 20 (2009): 1092-1098.
9. Piscopo G, Pezzuti E, Valentini PP, Three-Dimensional Finite-Element Analysis of Immediate Loading Dental Implants. J Biomech Sci Eng 3 (2008): 312-323.
10. Tseng CG, Jiang YS, Shih KS, Mechanics Comparison of Various Designs of Implant-supported Mandibular Restoration. J Biomech Sci Eng 3 (2008): 275-286.
11. Rubo JH, Souza EA, Finite element analysis of stress in bone adjacent to dental implants. J oral implantol 34 (2008): 248-255.
12. Maezawa N, Shiota M, Kasugai S, Wakabayashi N, Three-dimensional stress analysis of tooth/implant-retained long-span fixed denture. Int J Oral Maxillofac Implants 22 (2007): 710-718.
13. Bellini CM, Romeo D, Galbusera F, Taschieri S, Raimondi MT, Zampelis A, Francetti L, Comparison of tilted versus

nontilted implant-supported prosthetic designs for the restoration of the edentuous mandible: a biomechanical study. Int J Oral Maxillofac Implants 24 (2009): 511-517.

14. Zarone F, Apicella A, Nicolais L, Aversa R, Sorrentino R, Mandibular flexure and stress build-up in mandibular full-arch fixed prostheses supported by osseointegrated implants, Clin Oral Implants Res 14 (2003): 103-114.
15. Din X, Zhu XH, Liao SH, Zhang XH, Chen H, Implant-bone interface stress distribution in immediately loaded implants of different diameters: a three-dimensional finite element analysis. J Prosthodont 18 (2009): 393-402.
16. Seong WJ, Kim UK, Swift JQ, Heo YC, Hodges JS, Ko CC, Elastic properties and apparent density of human edentulous maxilla and mandible. J Oral Maxillofac Surg 38 (2009): 1088-1093.
17. Adell R, Lekholm U, Rockler B, Branemark PI, A 15-yuar study of osseointegrated implants in the treatment of the edentulous jaw. Int J Oral Surg 10 (1981): 387-416.
18. Keyak JH, Rossi SA, Jones KA, Skinner HB, Prediction of femoral fracture load using automated finite element modeling. J Biomech 31 (1998): 125-133.
19. Todo M, Biomechanical analysis of hip joint arthroplasties using CT-image based finite element method. J Surg Res 1 (2018): 34-41.
20. Ong KL, Kurtz SM, Manley MT, Rushton N, Mohammed NA, Field RE, Biomechanics of the Birmingham hip resurfacing arthroplasty. J Bone Joint Surg B 88 (2006): 1110-1115.
21. Teoh SH, Chui CK, Bone material properties and fracture analysis: Needle insertion for spinal surgery. J Mech Behav Biomed Mater 1 (2008): 115-139.
22. Reina JM, Garcia-Aznar JM, Dominguez J, Doblare M, Numerical estimation of bone density and elastic constants distribution in a human mandible. J Biomech 40 (2007): 828-836.
23. Yu HS, Baik HS, Sung SJ, Kim KD, Cho YS, Three-dimensional finite-element analysis of maxillary protraction with and without rapid palatal expansion. Eur J Orthod 29 (2007): 118-125.
24. Akca K, Iplikcioglu H, Finite element stress analysis of the effect of short implant usage in place of cantilever extensions in mandibular posterior edentulism. J Oral Rehabil 29 (2002): 350-356.
25. Ziebowicz A, Marciniak J, The use of miniplates in mandibular fractures: biomechanical analysis. J Mater Process Technol 175 (2006): 452-456.
26. Reimann S, Keiling L, Jager A, Bourauel C, Biomechanical finite-element investigation of the position of the centre of resistance of the upper incisors. Eur J Orthod 29 (2007): 219-224.
27. Daas M, Dubois G, Bonnet AS, Lipinski P, Rignon-Bret C, A complete finite element model of a mandibular implant-retained overdenture with two implants: Comparison between rigid and resilient attachment configurations. Med Eng Phys 30 (2008): 218-225.
28. Boccaccio A, Prendergast PJ, Pappalettere C, Kelly DJ, Tissue differentiation and bone regeneration in an osteotomized mandible: a computational analysis of the latency period. Med Biol Eng Comput 46 (2008): 283-298.
29. Chou HY, Jagodnik JJ, Muftu S, Predictions of bone remodeling around dental implant systems. J Biomech 41 (2008): 1365-1373.
30. Weinans H, Huiskes R, Grootenboer HJ, The behavior of adaptive bone-remodeling simulation models. J Biomech 25 (1992): 1425-1441.
31. Eser A, Tonuk E, Akca K, Cehreli MC, Predicting time-dependent remodeling of bone around immediately loaded dental

implants with different designs. Med Eng Phys 32 (2010): 22-31.

32. Qian L, Todo M, Matsushita Y, Koyano K, Finite Element Analysis of Bone Resorption Around Dental Implant. J Biomech Sci Eng 4 (2009): 365-376.
33. Huiskes R, Weinans H, Grootenboer HJ, Dalstra M, Fudala B, Slooff TJ, Adaptive bone-remodeling theory applied to prosthetic-design analysis. J Biomech 20 (1987): 1135-1150.
34. Tsubota K, Suzuki Y, Yamada T, Hojo M, Makinouchi A, Adachi T, Computer simulation of trabecular remodeling in human proximal femur using large-scale voxel FE models: Approach to understanding Wolff's law. J Biomech 42 (2009): 1088-1094.
35. Tawara D, Sakamoto J, Oda J, Finite element analysis considering material inhomogeneousness of bone using "ADVENTURE system". JSME Int J C : Mech Syst Mach Elements and Manuf 48 (2005): 292-298.
36. Mericske-Stern R, Assal P, Mericske E, Bürgin W, Occlusal force and oral tactile sensibility measured in partially edentulous patients with ITI implants. Int J Oral Maxillofac Implants 10 (1995): 345-353.

**Citation:** Takaaki Arahira, Mitsugu Todo. Biomechanical Study of Implant Treatment For Maxillas With Different Bone Quality. Dental Research and Oral Health 2 (2019): 003-016.